

# Influence of Impulse Wave Front Time on Flashover Characteristics of Coaxial Bus line of 220kV GIS

Lingli Zhang, Xuandong Liu, Can Guo, Ming Chen, Tao Wen, Qiaogen Zhang  
 High Voltage Division  
 School of Electrical Engineering, Xi'an Jiaotong University  
 Xi'an, 710049, China

**Abstract**—In order to find out the detection effectiveness of GIS insulation defects when suffering different overvoltages, a coaxial bus line of 220kV with a needle attached to it was established as an experimental sample to simulate the practical condition that there existed a metallic particle on the bus line of real GIS. Research was carried on with the help of 1MV steep-fronted impulse generator. By changing the wave front resistance of Marx generator, different kinds of double exponential impulse voltages could be produced. Influence of wave front time ( $t_f$ ) on 50% discharge voltage ( $U_{50}$ ) and voltage-time ( $v-t$ ) characteristic of GIS was studied in this article. Results indicate that with  $t_f$  increasing,  $U_{50}$  presents an increasing tendency overall; with pressure ( $P$ ) increasing, when  $t_f$  is short,  $U_{50}$  hardly changes with  $P$ , but when  $t_f$  becomes long enough,  $U_{50}$  changing with  $P$  appears as a hump curve. As for  $v-t$  characteristic, it turns out that, with the length ( $l$ ) of needle decreasing, both breakdown voltage and its dispersibility increase; it's also found that the shorter the needle is, the shorter delay that turning point occurs becomes. When  $t_f$  changes, shape of  $v-t$  characteristic changes too, the  $v-t$  characteristic integration of different wave front times looks like a concave basin. The above phenomena are explained in the view of the ionization, diffusion and recombination of space charges.

**Keywords**—Gas-insulated metal-enclosed switchgear (GIS); wave front time ( $t_f$ ); 50% discharge voltage ( $U_{50}$ ); voltage-time ( $v-t$ ) characteristic; space charges

## I. INTRODUCTION

SF<sub>6</sub> has been widely used as insulating gas in high voltage electrical equipment since 1940s due to its excellent performance. The gas-insulated metal-enclosed switchgear (GIS) appeared in 1965. GIS has lots of advantages such as compact structure, high reliability, flexible configuration and high security, and it's widely applied in power system at home and abroad [1-2].

The insulation system of GIS is mainly constituted by gas, and the pros and cons of insulation performance are important indicators to evaluate the reliability of GIS [3]. As voltage level of power system increases continually, more insulation breakdown accidents caused by GIS internal insulation defects occur, and they have a severe deterioration on safe and stable operation of power system. GIS has a quasi-uniform electric field structure macroscopically. However, dust or conductive particles may intrude into GIS during operating. What's more, improper operation and bump may exist during the process of transportation or assembly and disassembly. As a result,

defects might occur in inner part of GIS inevitably. These defects will distort partial electric field, reduce insulating property and eventually endanger the security of power system and power quality [4-8].

GIS in operation may suffer from overvoltages with different waveform parameters [9-10]. Once insulation defects appear, GIS will be high likely to operate accidently. Therefore, influence of impulse wave front time on flashover characteristics of GIS was studied in this article, including 50% discharge voltage and voltage-time characteristic, to find out the conditions of GIS insulation defects when they suffered different overvoltages.

## II. THE EXPERIMENTAL DEVICE AND METHOD

Experiment was carried on with the help of 1MV steep-fronted impulse generator, which is shown in figure 1. By changing the wave front resistance of Marx generator, different kinds of double exponential impulse voltages were produced [11], whose half-value time was 46.5μs, and wave front times were respectively 0.08, 0.40 and 0.90 μs, which are shown in figure 2.

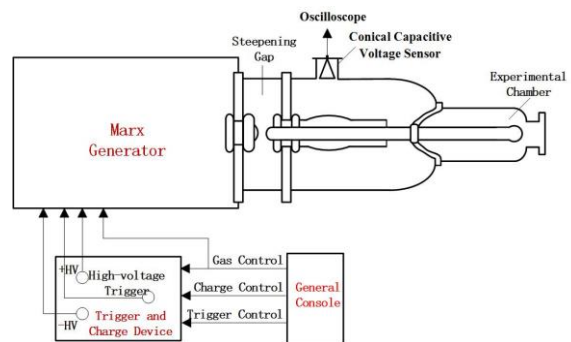
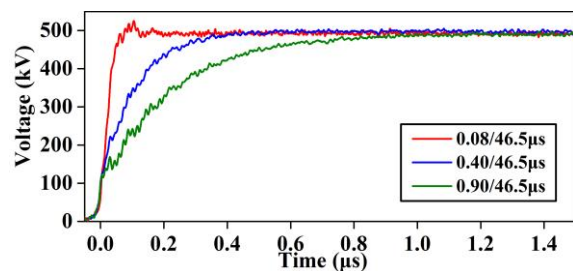
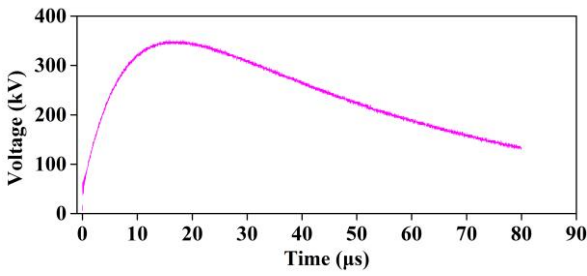


Fig.1. Configuration of 1MV steep-fronted impulse generator



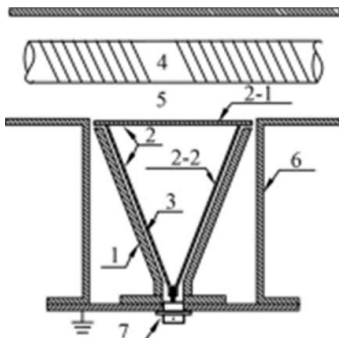
(a) wave front times are respectively 0.08μs, 0.40μs and 0.90μs



(b) wave front time is 15μs

Fig.2. Double exponential impulse voltages with different wave front times

The experimental measuring system consisted of conical capacitive voltage sensor, double shielded cable, coaxial integrator and oscilloscope, and configuration of conical capacitive voltage sensor is shown in figure 3.



1: outer cone 2-1: induction electrode 2-2: inner cone 3: polyimide film  
 4: high voltage bus line of GIS 5: SF<sub>6</sub> 6: shell 7: BNC joint  
 Fig.3. Configuration of conical capacitive voltage sensor

Experimental model in this article was a coaxial bus line in 220kV GIS, an all steel needle was attached to the high voltage bus line to simulate a metallic conducting particle in actual condition. Lengths of needles were respectively 3mm, 5mm, and 10mm. The point of needle was very fine, and its radius of curvature was about 100μm. The electrode structure can be seen in figure 4.

By changing  $t_f$  of double exponential impulse voltage, influence on flashover characteristics, including  $U_{50}$  and  $v-t$  characteristic, could be studied. During experiments, positive impulse voltage was applied to experimental model due to its lower breakdown voltage compared with that under negative impulse in terms of this electrode structure, which is beneficial for fault detection.

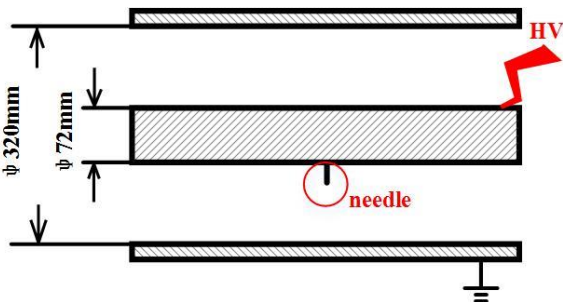


Fig.4. Coaxial bus line with protrusion attached to it

### III. EXPERIMENTAL RESULT

#### A. Influence of Wave Front Time on the 50% discharge voltage

When  $t_f$  is changed,  $U_{50}$  of coaxial bus line with a needle attached to it presents an increasing tendency overall, the change law can be seen in figure 5. Pressure of SF<sub>6</sub> in experiment is fixed to 0.6 MPa.

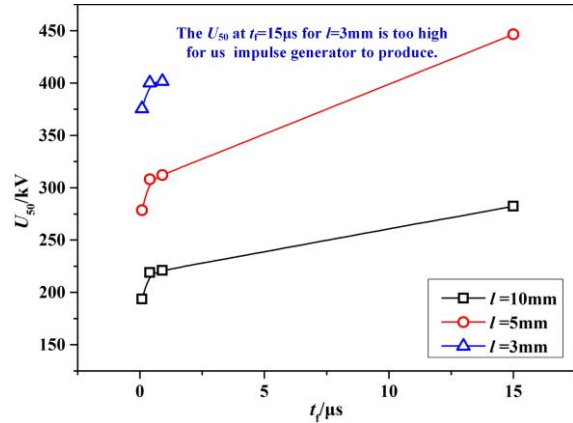
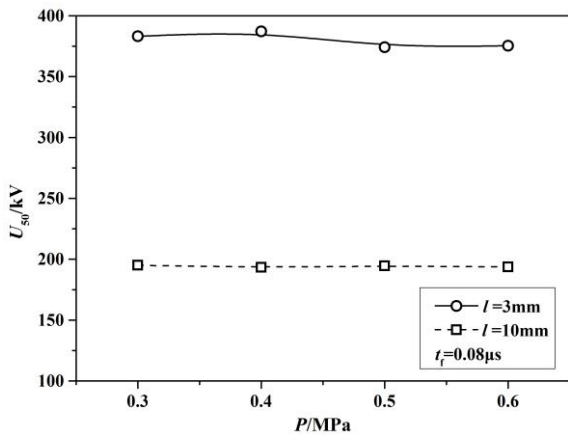


Fig.5. Influence of  $t_f$  on  $U_{50}$

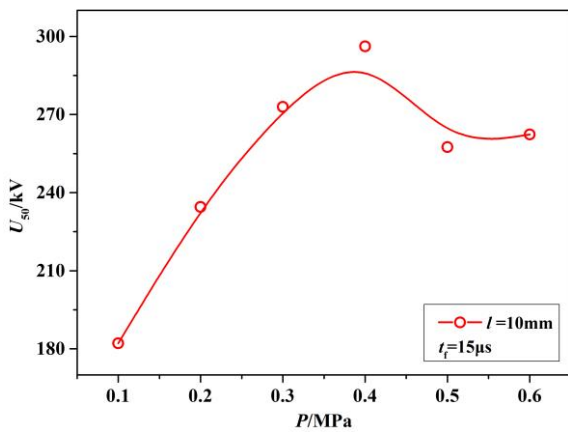
The electric field is a quasi-uniform field as a whole because of the electrode chosen in this experiment, only in the vicinity of needle tip, electric field is seriously distorted. As a result, discharge will always develop from the needle tip. From figure 5, it can be seen that with  $t_f$  increasing,  $U_{50}$  firstly increases rapidly and then slowly. It can be speculated that when  $t_f$  is long enough,  $U_{50}$  may finally approach a saturation value under sustained-action voltage. As is known that the electric field near needle tip is nonuniform, there must be a corona before breakdown, and space charges produced by corona discharge will further change the electric field near needle tip and then influence breakdown voltage [12]. When  $t_f$  is short, space charges have no time to move far, so they barely have effect on breakdown, and  $U_{50}$  is relatively low. But with  $t_f$  increasing, space charges move away from the tip and can improve the distribution of electric field, which is called “corona stabilization” effect, and as a result,  $U_{50}$  increases with  $t_f$  increasing. However, after moving a certain distance, corona stabilization effect gradually becomes stabilized, and growth rate of  $U_{50}$  slows down too. During the experiment, the turning point is about 0.4μs.

Under double exponential impulse voltage with different wave front times,  $U_{50}$  changing with pressure is also studied. The experimental results show that  $U_{50}$  hardly changes with pressure when  $t_f$  is short, but once  $t_f$  gets long enough,  $U_{50}$  changing with pressure appears as a hump curve. Take 0.08μs and 15μs as two typical wave front times, the phenomenon can be seen in figure 6.

As is shown in fig.6 (a), when pressure of SF<sub>6</sub> changes from 0.3MPa to 0.6MPa,  $U_{50}$  hardly changes as  $t_f$  is 0.08μs. As mentioned above, when  $t_f$  is very short, space charges produced by corona discharge have no time to move, they have no effect



(a)  $t_f=0.08\mu s$



(b)  $t_f=15\mu s$

Fig.6. Influence of pressure on  $U_{50}$

on breakdown voltages. At this time, leader discharge in a nonuniform electric field determines  $U_{50}$ . Previous studies have shown that the electric field strength of leader channel is rather low, about several kV/cm, and it will not change with pressure. So  $SF_6$  gap breaks down once the conditions of lead formation are met, and it's independent of pressure. However, when  $t_f$  becomes long enough, influence of space charges can't be ignored any more. In fig.6 (b),  $U_{50}$  changing with pressure appears as a hump curve. Under lower pressure, streamers occur and form a corona from which, however, leaders can not start because the shielding effect of corona space charges [13-14]. As a result, breakdown is determined by streamers and  $U_{50}$  rises with pressure increasing. When  $U$  exceeds a certain value, leader onset criterion is fulfilled, and breakdown is determined by leaders.  $U_{50}$  is reduced for a low electric field strength of leader channel and it changes little with pressure.

### B. Influence of Wave Front Time on the voltage-time characteristic

To have a more comprehensive understanding of impulse breakdown characteristics of  $SF_6$  coaxial gap, voltage-time characteristic changing with lengths of needle is studied at the condition that wave front time is  $0.08\mu s$  and pressure is  $0.6MPa$ .

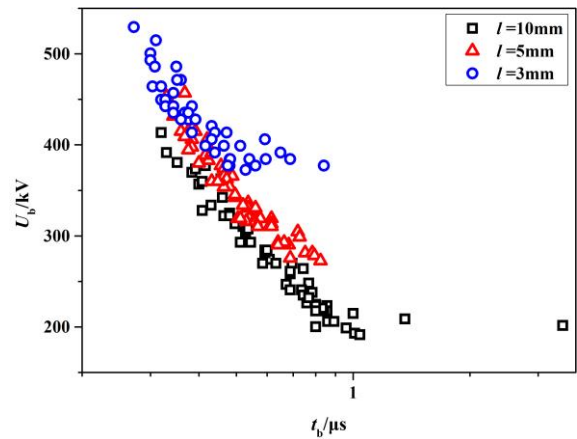
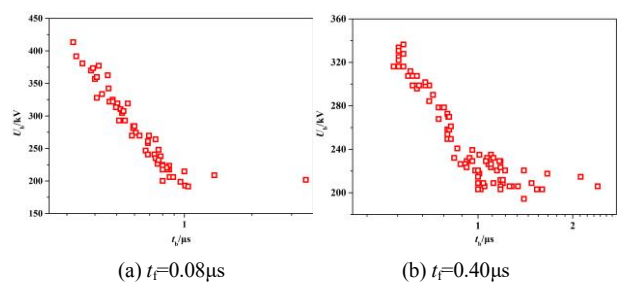


Fig.7. Influence of the length of needle on  $v-t$  characteristic

It can be seen from figure 7 that with the length ( $l$ ) of needle becoming longer, breakdown voltage decreases and its dispersibility is reduced. When  $l$  gets longer, electric field shielding effect of high voltage bus line is weakened, so the distribution of electric field near needle tip becomes more nonuniform. This condition of partial electric field concentration is beneficial for emitting electrons and then producing an effective initial one, that is to say, statistical delay becomes small. In  $SF_6$ , the dispersibility of breakdown mainly depends on its statistical delay, therefore, the dispersibility is reduced as  $l$  getting longer. What's more, it can be found that the shorter the needle is, the shorter delay that turning point occurs becomes. We can take the turning point as a result of space charges. Before turning point occurs, discharge delay plays an important role on breakdown. As the development of discharge requires a certain time delay, breakdown voltage increases with the shortening of discharge time. However, after turning point appears, influence of space charges becomes prominent. Space charges move a certain distance so that they can improve the distribution of electric field, then breakdown voltage doesn't drop any more. When  $l$  gets longer, it's essential for space charges to move farther to work, so the turning point appears in a longer delay region too. It is worth mentioning that when  $t_f$  is short, there are actually a few space charges in discharge area, so the turning point is not very distinct.

Voltage-time characteristic changing with  $t_f$  is also studied. The flowing fig.8 (a) to fig (d) show voltage-time characteristic when  $t_f=0.08\mu s$ ,  $t_f=0.40\mu s$ ,  $t_f=0.90\mu s$ , and  $t_f=15.0\mu s$  respectively. Figure 9 shows integration of voltage-time characteristic obtained under the action of double exponential impulse voltage of different wave front times.



(a)  $t_f=0.08\mu s$

(b)  $t_f=0.40\mu s$

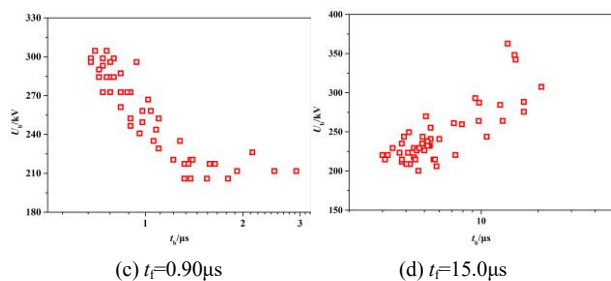


Fig.8. Influence of  $t_f$  on  $v-t$  characteristic

It can be found from figure 8 that when  $t_f$  changes, shape of voltage-time characteristic changes too. When  $t_f$  is  $0.08\mu s$ , the shape looks like a belt obliquing to the top left. With  $t_f$  increasing, the belt has a turning point, and breakdown occurring after turning point becomes more. When  $t_f$  lasts up to  $15\mu s$ , the belt totally obliquates to the right top. As is shown in figure 9, the voltage-time characteristic integration of different wave front times is like a concave basin, both sides tilt outside and the central part remains flat. The first three pictures in figure 8 can be considered to be a result of the combined effect of discharge time delay and space charges. The last picture, when  $t_f$  is  $15.0\mu s$ , as breakdown time increasing, gap discharge voltage rises as a whole. This can be explained from the following two aspects. Firstly, the voltage application duration is long enough to clean initial space charges, that is, the initial positive and negative ions move to anode or cathode under the action of electric field force in voltage rise phase [15]. It's difficult to generate an effective initial electron, so breakdown voltage is high. Secondly, "corona stabilization" effect improves electric field distribution around needle tip and then improves the breakdown voltage to a certain extent.

What's more, when  $t_f$  becomes longer, voltage rise rate is slow, after electrons appear, they may recombine with each other, or migrate out of gap, or terminate ionization. That is to say, statistical delay becomes large, so the dispersibility of discharge extend too, and the belt of voltage-time characteristic curve is widened.

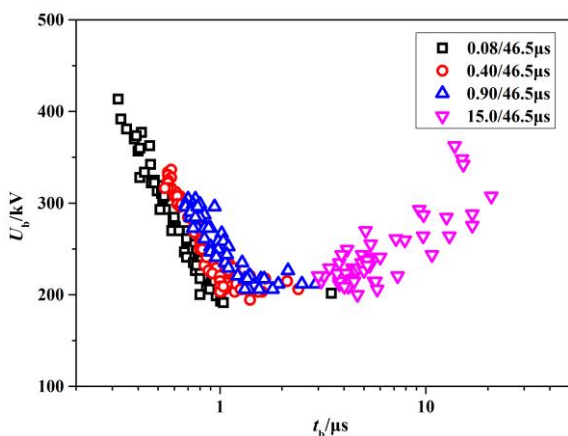


Fig.9.  $V-t$  characteristic integration of different wave front times

#### IV. CONCLUSION

- Under double exponential voltages with different wave front times, along with  $t_f$  increasing,  $U_{50}$  presents an increasing tendency overall. With pressure increasing,

when  $t_f$  is short,  $U_{50}$  remains stable, but when  $t_f$  becomes long enough,  $U_{50}$  appears as a hump curve.

- When studying voltage-time characteristic, with the length of needle decreasing, both breakdown voltage and its dispersibility increase; what's more, the shorter the needle is, the shorter delay that turning point occurs becomes.
- As wave front time changes, shape of voltage-time characteristic changes too, the voltage-time characteristic integration of different wave front times looks like a concave basin.

#### REFERENCES

- [1] YAN Zhang, ZHU Deheng. High voltage insulation engineering [M]. Beijing, China: China Electric Power Press, 2007.
- [2] ZHANG Lu. Study of discharge characters for typical insulation structure of GIS under very fast transient overvoltage [D]. Xi'an, China: School of Electrical Engineering, Xi'an Jiaotong University, 2014.
- [3] Riechert U, Holaus W. Ultra high-voltage gas-insulated switchgear-a technology milestone [J]. European Transactions on Electrical Power, 2012, 22(1): 60-82.
- [4] Zhang Q, Qiu Y, Wang P, et al. Dielectric characteristics of SF<sub>6</sub> under the steep-fronted impulses [C]. IEEE International Symposium on Electrical Insulation. 1996: 770-773 vol.2.
- [5] ZHANG Qiaogen, GU Wenguo. Insulating characteristics of SF<sub>6</sub> under the Steep-Fronted Impulses [J]. High Voltage Engineering, 1996(01): 6-8.
- [6] ZHANG Qiaogen, QIU Yuchang. Insulation characteristics of SF<sub>6</sub> gap under very fast transient overvoltage [J]. High Voltage Apparatus, 1995, 31(3): 38-43.
- [7] WEN Tao, ZHANG Qiaogen, MA Jingtian, et al. Influence of impulse waveform parameters on breakdown voltage in SF<sub>6</sub> Quasi-uniform electric field of rod-plate gap [J]. High Voltage Engineering, 2016, 42(3): 936-941.
- [8] LI Qingmin, WANG Jian, LI Botao, et al. Review on metal particle contamination in GIS/GIL [J]. High Voltage Engineering, 2016, 42(3): 849-860.
- [9] Okabe S, Tsuboi T, Ueta G. Study on lightning impulse test waveform for UHV-class electric power equipment [J]. IEEE Transactions on Dielectrics and Electrical Insulation, 2012, 19 (3): 803-811.
- [10] Okabe S, Yuasa, S, Kaneko, S. Evaluation of Breakdown Characteristics of Gas Insulated Switchgears for Non-Standard Lightning Impulse Waveforms - Breakdown Characteristics for Non-Standard Lightning Impulse Waveforms Associated with Lightning Surges [J]. IEEE Transactions on Dielectrics and Electrical Insulation, 2008, 15(3):407-415.
- [11] SHI Wei, QIU Yuchang, ZHANG Qiaogen. Fundamental of high voltage engineering [M]. Beijing, China: China Machine Press, 2006.
- [12] WANG Lei, CHEN Weijing, YUE Gongchang, et al. Simulation Analysis of Potential Caused by Trapped Charge in Disconnecter of UHV Gas Insulated Switchgear Device [J]. High Voltage Engineering, 2014, 40(12): 3911-3917.
- [13] CAI Xinjing, WANG Xinxin, ZOU Xiaobing, et al. Properties of Streamer Discharges in Different Gases at Atmospheric Pressure [J]. High Voltage Engineering, 2015, 41(6): 2047-2053.
- [14] F Pinnekamp, L Niemyer. Qualitative model of breakdown in SF<sub>6</sub> in inhomogeneous gaps [J]. J. Phys. D: Appl. Phys., 16 (1983) 1293-1302.
- [15] WEN Tao, ZHANG Qiaogen, ZHAO Junping, et al. On-site Test Technology of Standard Lightning Impulse for Power Equipment with Large Capacitance [J]. High Voltage Engineering, 2016, 42(9): 2968-2973.